

We are IntechOpen, the world's leading publisher of Open Access books Built by scientists, for scientists

4,800

Open access books available

122,000

International authors and editors

135M

Downloads

Our authors are among the

154

Countries delivered to

TOP 1%

most cited scientists

12.2%

Contributors from top 500 universities



WEB OF SCIENCE™

Selection of our books indexed in the Book Citation Index
in Web of Science™ Core Collection (BKCI)

Interested in publishing with us?
Contact book.department@intechopen.com

Numbers displayed above are based on latest data collected.
For more information visit www.intechopen.com



Blue Shift in the Spectrum of Arrival Times of Acoustic Signals Emitted during Laboratory Hydraulic Fracturing

Arcady V. Dyskin, Elena Pasternak,
Andrew P. Bungler and James Kear

Additional information is available at the end of the chapter

<http://dx.doi.org/10.5772/56448>

Abstract

We discuss a method of detecting localised fracturing that potentially requires only one channel. The method is based on the notion that the fracture propagation involves generation of acoustic events from its contour. It is proposed that the number of events (microcracks) generated at each step of fracture propagation could be proportional to the fracture size to a certain power called the localisation exponent. This dependence of the number of generated events on the fracture size (the event coherence) leads to a shift to higher frequency (the “blue shift”) in the combined spectrum of the events as compared to the spectrum of randomly generated events. This concept was applied to the results of a laboratory test in which hydraulic fracture was driven by injecting glycerine into a 200x200x120mm block of polycrystalline gabbro. We show that there is indeed a blue shift in the spectrum of the arrival times at any one sensor that seems to correspond with the growth of a localized hydraulic fracture. The localisation exponent is able to distinguish between the cases of the fracture contour length roughly proportional to, and more slowly than proportional to, the nominal fracture radius.

1. Introduction

Hydraulic fracturing is a technique often used in subsurface geotechnical engineering for production stimulation in petroleum and geothermal reservoirs, for caving stimulation in the mining industry, and for stress measurements in the Earth’s crust. Since the size and orientation of the hydraulic fracture and the number of fractures induced by a given injection depend on potentially complicated conditions of rock mass structure and the stress state, they are often

difficult to predict. This necessitates the development of methods for detecting the geometry and location of the hydraulic fracture(s) and/or monitoring the process of its propagation. A number of methods were proposed for this purpose (see review [1]). They include treating pressure response (e.g. [2, 3]), tracing the fracture fluid (e.g. [3]), microseismic mapping (e.g. [1, 4-8]), crosswell seismic detection (e.g. [9, 10]), vertical seismic profiling (e.g. [11, 12]), borehole overcoring [1], borehole cameras (e.g. [13]), surface tilts (e.g. [8, 14, 15]).

The methods based on microseismic monitoring are attractive because they are capable of providing real-time information about the growth of the region that is impacted by stress and pore pressure changes that lead to the release of seismic energy during injection. Currently these methods are based on locating the microseismic events. Accurate locations of the sources require simultaneous, recording the events using multiple sensors together with accurate measurements of the wave propagation velocities in multiple directions in the rock mass.

In contrast, Pasternak and Dyskin [16] proposed a method of detecting the localised fracturing which potentially requires only one channel. The method is based on the notion that the propagation of a localised fracture process (e.g., the process zone of the hydraulic fracture) involves generation of microcracks from the contour of a propagating localised zone or a fracture. The microcrack generation is almost instantaneous as compared to the time of crack propagation since the interaction between the main fracture or localisation zone and the microcracks occurs with the speed of the stress waves. As a result the number of events (microcracks) generated at each step of fracture propagation should be proportional to the length of the contour and hence proportional to the radius of the propagating fracture. This dependence of the number of generated events on the fracture radius (the event coherence) leads to the blue shift (i.e. shift to higher frequencies) in the combined spectrum of the events as compared to the spectrum of randomly generated events. The blue shift can even be detected in the 'spectrum of arrival times' that is the Fourier transform of the time delays between the arriving signals.

Obviously single sensor data will never lead to event locations. Instead, the goal of the Blue Shift approach is to enable using a relatively inexpensive single sensor array in order to detect localization and, ultimately, to be able to infer something about the dimensionality of the leading edge of the fracture. We hope to distinguish among, for example: 1) height constrained (i.e. PKN) type growth where the length of the propagating leading edge is essentially fixed at the height of the reservoir, 2) quasi-radial growth where the length of the leading edge grows proportionally to the nominal radius, and 3) diffuse or network-type growth where the combined length of the fractures' leading edges grows more rapidly than proportionality to the nominal radius of the fractured zone.

In this paper we report the results of a first-stage laboratory test conducted in order to provide guidance to the ongoing development of the Blue Shift approach. The following section, Section 2 describes the essentials of this approach. Section 3 describes the experiments and the measurements and Section 4 shows the application of the blue shift indicator to analyse the recorded acoustic emission.

2. Blue shift indicator

Consider a hydraulic fracture, which propagates emitting acoustic pulses from its process zone that is small compared to the fracture size $R(t)$, Figure 1. We do not specify the particular shape of the fracture as long as it propagates in plane in all directions and its diameter and perimeter are proportional to the size, R . It is natural to assume that the hydraulic fracture is produced in quasi-static regime, that is the time intervals between successive steps of fracture propagation are considerably larger than the time needed for the stress waves to traverse the process zone along the contour of the fracture and effect the interaction between the acoustic events. Similarly, it is natural to assume that the time step of fracture propagation is much larger than the time needed for the acoustic signal to reach the acoustic sensor such that one can regard the signal emitted at one step of fracture propagation as being received almost simultaneously.

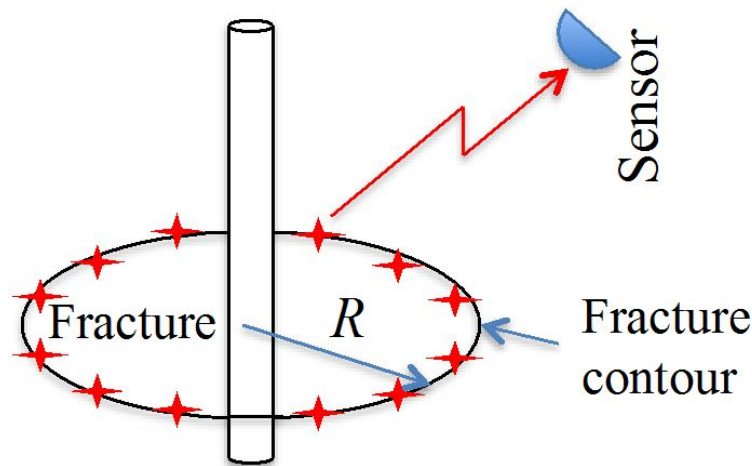


Figure 1. Hydraulic fracture and acoustic events at its contour produced almost simultaneously during a step in fracture propagation.

Suppose we have recorded a set of arrival times $\Theta = \{t_1, t_2, \dots, t_M\}$, where M is the number of generated acoustic pulses. Then, according to [16], we can regard t_k as a time shift with respect to zero and relate the Fourier transform $\exp(-i\omega t^k)$ to it. We compute the 'spectrum' of arrival times by adding their Fourier transforms and calculate the energy the spectrum possess in the frequency range $(0, \Omega)$, where Ω is a certain frequency. The blue shift indicator is a measure of the difference between the energy associated with arrival times synchronised due to the localisation and purely random arrival times:

$$\Sigma_n(M, \Theta, \Omega) = \frac{|S(M, \Theta, \Omega) - S_r(M, \Omega)|}{S_r(M)} \quad (1)$$

where the 'energies' of the truncated spectrum (up to frequency Ω) of arrival times Θ and the random arrival times $\{t_k^{(r)}\}$ are

$$S(M, \Theta, \Omega) = (M - 1)\Omega + 2 \sum_{m=2}^M \sum_{l=1}^{m-1} \frac{\sin((t_m - t_l)\Omega)}{t_m - t_l} \quad (2)$$

$$S_r(M, \Omega) = \int_0^{\Omega} \sum_{k,l=0}^M \exp[-i(t_k^{(r)} - t_l^{(r)})] d\omega \quad (3)$$

We assume that the fracture propagation proceeds stepwise. It was shown in [16] that it is sufficient to assume that all steps take the same time ΔT . At each time step the nominal fracture radius increases by ΔR . We initially assume that the number of pulses emitted is proportional to the crack perimeter, that is at k -th step the number of pulses emitted is equal to pk , where p is a factor accounting for the particular fracture shape and the relative distance between the locations of the acoustic events in each step. (Section 5 will check this assumption.) Let the time of the beginning of the propagation step k be $k\Delta T$. Then we can assign the theoretical value of the blue shift indicator by applying (1)-(3) to the 'recorded' sequence of arrival times that consists of pk^α arrival times randomly distributed within the interval $(k\Delta T, (k+1)\Delta T)$. Here in the ideal case, the localisation exponent $\alpha=1$ since the circumference of the fracture is proportional to the step number. We however would like to allow for a possibility of either varying steps of fracture expansion or a fractal nature of the set of defects generated by crack growth and therefore will allow for different values of α .

We note that the number of 'recorded' and random arrival times are proportional to p . Therefore, in the formula for the blue shift indicator (Eq. 1), p will cancel out. Hereafter, without loss of generality, we assume $p=1$.

3. Laboratory tests

In order to provide initial verification and to guide ongoing development of the analysis, a laboratory test was conducted in which a hydraulic fracture was driven by injecting glycerine into a 200x200x150mm block of polycrystalline gabbro. Acoustic emissions were detected and located based on their arrival times to 32 transducers that were attached to the 6 faces of the block. After testing, the specimen was serial sectioned so that fracture patterns could be observed and measured, see the example in Figure 2.

In total, 463 events were located with <2 mm uncertainty. Events that were not able to be located within the block to this level of accuracy were discarded, as the source of such events is not certain. Figure 3 shows these events as they occurred in time while Figure 4 shows the pressure record along with the cumulative events. In total, 70 events occurred before the hydraulic fracture was observed to have intersected the edge of the specimen ("breakthrough") and fluid was seen to be slowly leaking from the side of the specimen through the crack. An additional 160 events were recorded before shut-in and the remaining, post shut-in events are essentially



Figure 2. Example of serial sectioned hydraulic fracture showing growth from a notch in a 16 mm diameter wellbore.

aftershocks that we believe to be similar to those observed in experiments on rock failure in compression [17] and in other hydraulic fracturing laboratory experiments [18].

4. Blue shift indicator for the experimental data

The 70 events recorded prior to fracture breakthrough at the specimen edge are not a sufficient number for blue shift calculations. So instead we conducted the analysis for the first 200 and for all 463 events. That means that the first group contains a larger proportion of events produced from a contour of fracture during the time it was growing in quasi-planar manner with a leading edge that is a circumscribing line, that is, when localisation exponent $\alpha \approx 1$. The second group contains a smaller proportion of propagation-related events. If the contour length is constant then $\alpha = 0$, therefore in the case of all events one can expect $0 < \alpha < 1$ and we certainly would expect the second group to have a smaller exponent than the first.

Figure 5 shows the blue shift indicator for the first 100 and first 200 and for all 463 events, respectively, compared with theoretical values for different localisation exponents where the particular values of the exponent were chosen to ensure the best fit. It is seen that the experimental blue shift curves have the characteristic peaks indicating, according to [16], the presence of localisation. For the group of first 100 events (Figure 5a) the best fit curve corresponds to the localisation exponent $\alpha = 0.97$, which is close to the expected $\alpha = 1$. For the group of 200 events (Figure 5b) the best fit exponent is $\alpha = 0.37$. Interestingly using all 463 events (Figure 5c) does not change the best fit exponent. The localisation exponent for 200 and 463 events is within the expected boundaries $0 < \alpha < 1$ and, as anticipated, it is less than the exponent obtained from the first group. According to the Blue Shift approach, this smaller exponent is indicative that a smaller proportion of the events are associated with localized crack growth at the fracture's leading edge. This is indeed seen in the difference between 200 (Figure 5b) and 463 (Figure 5c) events when the adding the events unrelated to the localised process of the fracture growth does not affect the exponent but decreases the accuracy of the fit.

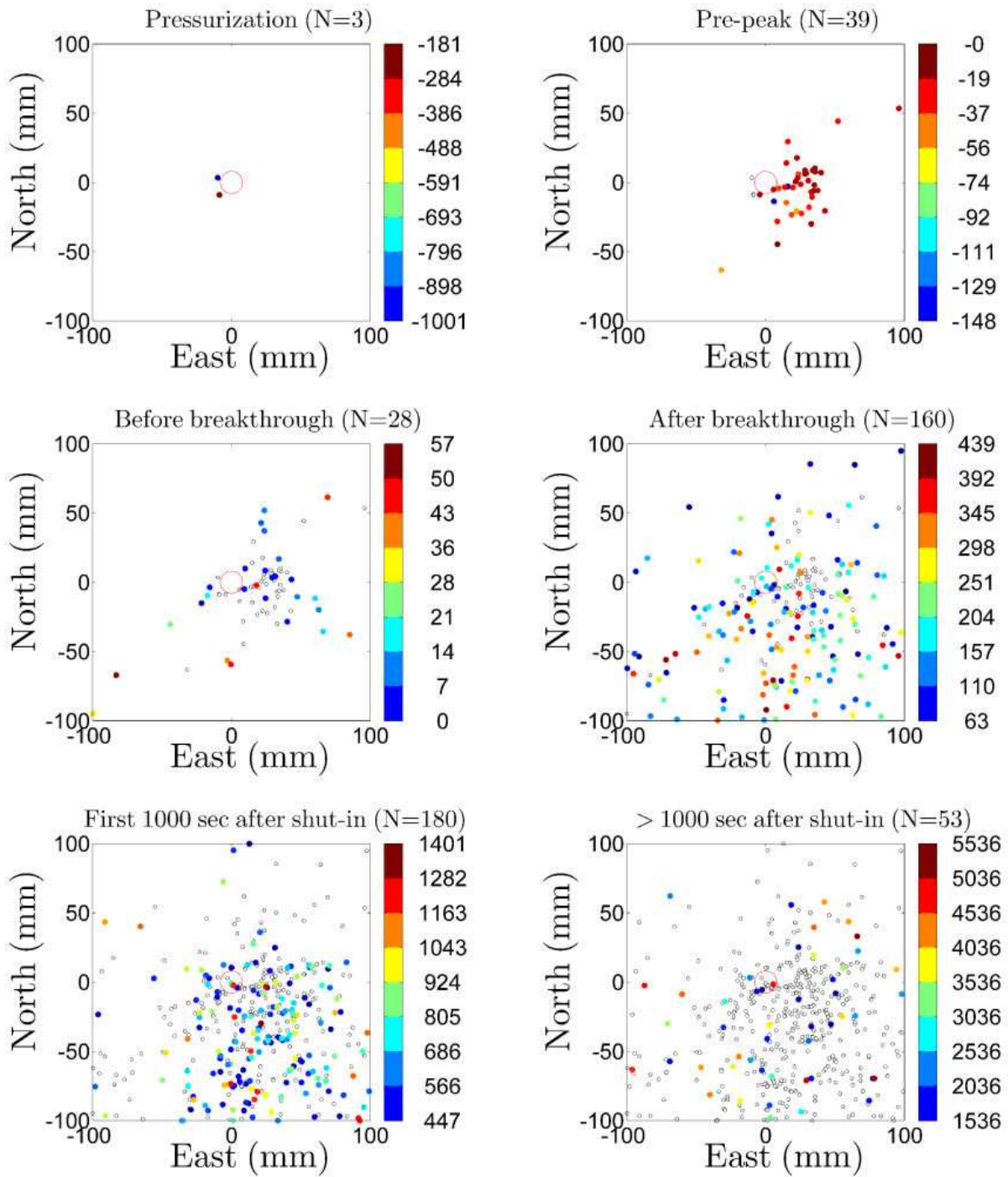


Figure 3. Acoustic emissions detected with <2mm location uncertainty. Colour corresponds to time measured from the time of the peak pressure. Open circles indicate events that occurred at a previous time range. Breakthrough refers to the time at which the hydraulic fracture was observed to have intersected the specimen boundary.

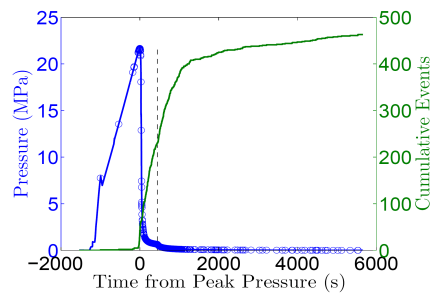


Figure 4. Evolution of injection pressure and cumulative number of events. Here the blue circles correspond to each event and the vertical dashed line indicates the time of shut-in.

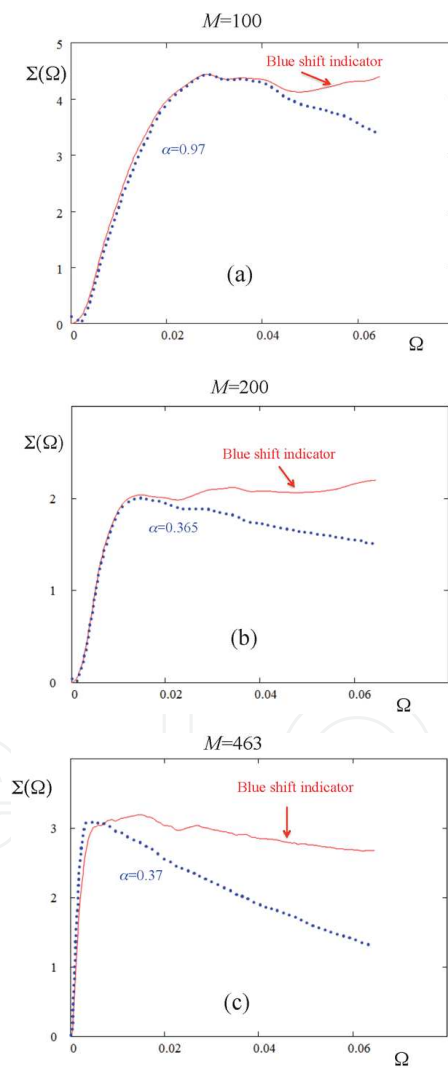


Figure 5. Blue shift indicators for the first 100 events (a), first 200 events (b) and all 463 events (c) recorded in the experiment compared with the best fit theoretical curves where the only fitting parameter is the localisation exponent.

5. Conclusions

Our results show an intriguing mix of promise and indication of challenges to be overcome. The results are promising in that the spectrum of the arrival times indeed undergoes a blue shift, the nature of which is notionally able to discern between the main localized, omnidirectional propagation stage and the period during which the propagation was arrested except, perhaps, for some slow growth that was directionally limited but during which most of the events were being generated from apparently spatially random locations around the vicinity of the fracture surface. What's more, the blue shift can be characterized by a parameter, the localisation exponent, which can theoretically be tied to the dimensionality of the leading edge of the hydraulic fracture.

However, we also discovered a preponderance of events that emit from the vicinity of the already-fractured surface rather than being localized at the leading edge. The impact of these non-localized events remains a topic for ongoing investigation. Hence, our ongoing work is aimed at providing a clear understanding of how experimentally derived values of the localisation exponent can be used to predict the fracture pattern associated with a given sequence of events.

Acknowledgements

The authors acknowledge support from the Capability Developments Funds of CSIRO Earth Science and Resource Engineering. AVD and EP acknowledge support from ARC Discovery Grant DP0988449.

Author details

Arcady V. Dyskin^{1*}, Elena Pasternak¹, Andrew P. Bungler^{2,3} and James Kear²

*Address all correspondence to: arcady.dyskin@uwa.edu.au

1 School of Civil and Resource Engineering, University of Western Australia, Crawley, Australia

2 CSIRO Earth Science and Resource Engineering, Melbourne, Australia

3 Department of Civil and Environmental Engineering, University of Pittsburgh, Pittsburgh, Pennsylvania, USA

References

- [1] Mahrer, K. D. A review and perspective on far-field hydraulic fracture geometry studies. *Journal of Petroleum Science and Engineering* (1999). , 24, 13-28.
- [2] Cleary, M. P, Doyle, R. S, Teng, E. Y, Cipolla, C. L, Meehan, D. N, Massaras, L. V, & Wright, T. B. Major new developments in hydraulic fracturing, with documented reductions in job costs and increases in normalized production. In: *Proceedings 69th Annual Technical Conference and Exhibition, New Orleans, LA.* (1994). , 1994, 547-561.
- [3] King, G. E. Tracking fracture fluid movement with chemical and gamma-emitting tracers with verification by microseismic recording. In: *EPA Hydraulic Fracturing Workshop, February* (2011). , 24-25.
- [4] Murphy, H. D, & Fehler, M. C. Hydraulic fracturing in jointed formations. In: *Proceedings Soc. Petr. Eng. International Meeting on Petroleum Engineering, Beijing, China.* (1986). , 1986, 489-496.
- [5] Mahrer, K. D. Microseismic logging: a new hydraulic fracture diagnostic method. *Soc. Petr. Eng. Form. Eval.* (1993). , 1993, 41-50.
- [6] Rutledge, J. T, & Zinno, R. J. Microseismic mapping of a Cotton Valley hydraulic fracture using decimated downhole arrays. *Society of Exploration Geophysicist, International Exposition and Sixty Eighth Annual Meeting, September 13- 18,* (1998).
- [7] Liu, X, Xu, Y. G, Zhao, Z. F, Mu, L. J, Liu, J. A, & Guo, Z. X. Application of microseismic mapping and modeling analysis to understand hydraulic fracture growth behaviour. *International Symposium and Exhibition on Formation Damage Control, February* (2006). Lafayette, Louisiana U.S.A. DOIMS., 15-17.
- [8] Cipolla, C. L, & Wright, C. A. Diagnostic Techniques to Understand Hydraulic Fracturing: What? Why? and How? *SPE/CERI Gas Technology Symposium, April* (2000). Calgary, Alberta, Canada. DOI:MS., 3-5.
- [9] Vinegar, H. J, Wills, P. B, Demartini, D. C, Shlyapobersky, J, Deeg, W. F. J, Adair, R. G, Woerpel, J. C, Fix, J. E, & Sorrells, G. G. Active and passive seismic imaging of a hydraulic fractures in diatomite. *J. Petr. Tech.* (1992).
- [10] Fehler, M, & Pearson, C. Cross-hole seismic surveys: applications for studying subsurface fracture systems at a hot dry rock geothermal site. *Geophysics* (1984). , 49, 37-45.
- [11] Meadows, M. A, & Winterstein, D. F. Seismic detection of a hydraulic fracture from shear-wave VSP data at Lost Hills Field, California. *Geophysics* (1994). , 59, 11-26.

- [12] Green, A. S. P, Baria, R, & Jones, R. VSP and cross-hole seismic surveys used to determine reservoir characteristics of a hot dry rock geothermal system. *Int. J. Rock Mech. Min. Sci. and Geomech. Abstr.* (1989). , 26, 271-280.
- [13] Palmer, I. D, & Sparks, D. P. Measurement of induced fractures by downhole TV camera in black warrior basin coalbeds. *J. Petr. Tech.* (1991).
- [14] Wright, C. A, & Conant, R. A. Hydraulic fracture reorientation in primary and secondary recovery from low-permeability reservoirs. In: *Proceedings Soc. Petr. Eng. Annual Technical Conference and Exhibition, Dallas, TX.* (1995). , 1995, 357-369.
- [15] Lecampion, B, Jeffrey, R, & Detournay, E. Resolving the Geometry of Hydraulic Fractures from Tilt Measurements, *Pure and Applied Geophysics* (2005). , 162, 2433-2452.
- [16] Pasternak, E, & Dyskin, A. V. Frequency signatures of damage localisation *Phil. Mag.* (2012).
- [17] Scholz, C. H. Microfractures, aftershocks, and seismicity. *Bull. Seis. Soc. America*, (1968). , 58(3), 1117-1130.
- [18] Chitrala, Y, Moreno, C, Sondergeld, C, & Rai, C. Microseismic and microscopic analysis of laboratory induced hydraulic fractures. In *Proceedings Canadian Unconventional Resources Conference, Calgary, Alberta, Canada, November* (2011). SPE 147321., 15-17.